Effect of Al Addition on Formation of Layer-Structured LiNiO$_2$

Shih-Pin Lin, Kuan-Zong Fung,[1] Yi-Ming Hon, and Min-Hsiung Hon

Department of Materials Science and Engineering, National Cheng Kung University, Tainan 70101, Taiwan

Kinetics and formation mechanism of undoped and Al-doped LiNiO$_2$ from Li$_2$CO$_3$ and NiO were investigated in this study. Without the addition of Al ions, sluggish kinetics for the formation of undoped LiNiO$_2$ was observed. The fraction of undoped LiNiO$_2$ reached 50% after Li$_2$CO$_3$ and NiO reacted at 700°C for 150 min. With the addition of 25% of Al ion, the fraction of Al-doped LiNiO$_2$ reached 50% within 60 min at 700°C. The analysis of kinetics study indicates that the formation of undoped and Al-doped LiNiO$_2$ is a diffusion-controlled process. Furthermore, the rate constant determined from Jander model $\{[1 - (1 - \alpha)^{1/3}]^2 = Kt\}$ was significantly enhanced by the addition of Al. The activation energy for the formation of LiNiO$_2$ drastically decreased from 190 kJ/mole (undoped reaction) to 83 kJ/mole when 25% Al was added. The enhancement of LiNiO$_2$ formation by Al doping is attributed to the structure resemblance between α-LiAlO$_2$ and LiNiO$_2$. α-LiAlO$_2$ acts as the seeding material which provides nucleation sites for the growth of LiNiO$_2$. © 2002 Elsevier Science (USA)

Key Words: **kinetics; lithium nickel aluminum oxide; cathode material.**

1. INTRODUCTION

The lithium transition-metal oxides, such as LiCoO$_2$, LiNiO$_2$, and LiMn$_2$O$_4$, have received a great deal of interest as rechargeable cathodes for Li secondary batteries (1–5). Among them, LiNiO$_2$ provides the advantage over LiCoO$_2$ system of being cost effective and environmentally safer.

LiNiO$_2$ is, however, known to exhibit thermal instability. For overcharged Li$_{1-x}$NiO$_2$, most of the Ni ions are in the unstable Ni^{4+} state which should be avoided (6). NiO$_2$ is quite active toward organic electrolyte oxidation. To solve the problems of unstable structure and thermal properties due to the formation of nickel dioxide, several cations, such as Al, Mn, and Co have been added into LiNiO$_2$ to

improve its thermal stability (7). Among them, Al doping has received much attention. The Al^{3+} ions tend to prevent the formation of nickel dioxide and promote the structural integrity.

It is well known that Li$_2$O and Al$_2$O$_3$ can form stable α-LiAlO$_2$ with the α-NaFeO$_2$ structure at temperatures below 600°C (8–10). The intercalation of α-LiAlO$_2$ gives a voltage of $\sim$5 V vs Li/ Li$^+$, which is higher than other lithium transition-metal oxides. Thus, the solid solution of α-LiAlO$_2$ with lithiated transition-metal oxide can potentially increase the intercalation voltage. Al doping was found to be an acceptable method to enhance the stability of LiNiO$_2$. In addition, α-LiAlO$_2$ also provides advantages of light weight, non-toxicity and low cost.

Most research related to Al-doped LiNiO$_2$ (11–14) has focused on electrochemistry, synthesis condition and/or structure of LiNiO$_2$. The formation mechanism and reaction kinetics of LiNiO$_2$ were seldom discussed. For undoped LiNiO$_2$, the solid-state reaction method has been studied with various Ni compounds such as Ni metal, Ni(OH)$_2$, NiCO$_3$, NiO, LiOH, and Li$_2$CO$_3$ reacted at temperatures ranging from 750 to 900 for 24–48 h (7, 15). Sluggish reactions were reported. Typically, it requires 48 h to obtain 100% LiNiO$_2$ at 800°C. With the addition of Al ions, the appearance of α-LiAlO$_2$ with high stability and low synthesis temperature may affect the formation of LiNiO$_2$ in a positive way. Therefore, the main objective of this work was to investigate the effect of Al ions on the synthesis mechanism and reaction kinetics of LiNiO$_2$ using Li$_2$CO$_3$ and NiO as the starting materials.

2. EXPERIMENTAL PROCEDURE

2.1. Sample Preparation

LiNiO$_2$ samples were prepared from lithium carbonate (99.7%, Fisher) and nickel oxide (99%, Alfa). Aluminum nitrate (98.5%, Riedel-deHaen) was added as the source of Al^{3+} for Al-doped LiNiO$_2$. The atomic ratio of Al/Ni varied from 0.1/0.9 to 0.25/0.75 accordingly. Starting

materials with desired ratio were wet mixed by ball milling for 24 h. For kinetics study, the powder mixture was dried and calcined at temperatures ranging from 650°C to 725°C for various periods of time from 15 min to 6 h, followed by quenching to room temperature. To ensure the complete reaction, some samples were also heated at temperatures as high as 800°C.

2.2. Characterization of Calcined $LiAl_xNi_{1-x}O_2$ Powder

X-ray diffraction (XRD) analysis was conducted on calcined powder using Rigaku X-ray Diffraction System (model D/MAX III.V) with monochromated Cu$K\alpha$ radiation. The accelerating voltage and current were set at 30 kV and 20 mA, respectively. A scan speed of 1°/min was selected from 10° to 80° of 2θ angles. The volume fraction (α) of LiNiO$_2$ was estimated from the consumption of NiO because the reflection intensity of LiNiO$_2$ was weak in the early stage of reaction. The volume fraction consumed was determined from integrated peak intensity of (002) reflection of NiO collected from 42.5° to 44.5° of 2θ angles in a step of 0.01° with a scan rate of 0.5°/min. The same procedure was also conducted on powder mixtures of NiO and LiNiO$_2$ with the volume fraction of NiO varying from 0%, 25%, 50%, 75% to 100%. The XRD traces obtained from these powder mixtures were used as standards. SEM observations were conducted using a PHILIPS XL 40 to examine the surface morphology of LiNiO$_2$ powder.
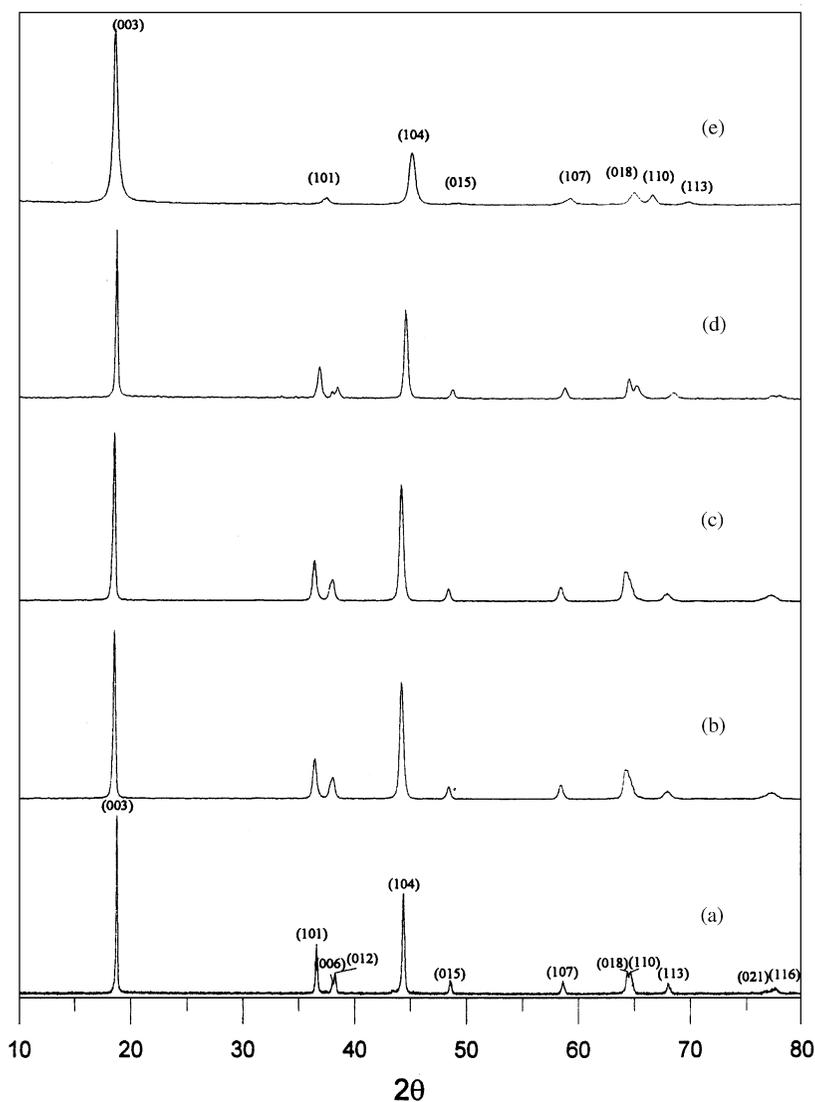
FIG. 1. The XRD patterns for LiAl$_x$Ni$_{1-x}$O$_2$ synthesized at 800°C for 54 h, when $x =$ (a) 0.00, (b) 0.10, (c) 0.20, (d) 0.25, and (e) LiAlO$_2$ synthesized at 500°C for 12 h.

3. RESULTS AND DISCUSSION

3.1. Structure Analysis of Undoped and Al-Doped $LiNiO_2$

Figure 1 exhibits the XRD patterns for α-$LiAlO_2$, undoped $LiNiO_2$, and Al-doped $LiNiO_2$ synthesized. All the samples were synthesized at 800°C for 54 h except α-$LiAlO_2$ which was synthesized at 500°C for 12 h. Both $LiNiO_2$ and α-$LiAlO_2$ exhibit a similar rhombohedral structure with a space group of $B\bar{3}m$. However, there exists variation in reflections of (006), (012), (018), and (110) between undoped $LiNiO_2$ and α-$LiAlO_2$. For α-$LiAlO_2$, the intensities for (006) and (012) reflections are negligible; the reflections of (018) and (110) are, however, clearly separated. On the other hand, the intensities for reflections of (006) and (012) of $LiNiO_2$ are noticeable. But, the reflections of (018) and (110) for $LiNiO_2$ are indistinguishable. The reasons for these variations can be explained by: (1) The difference in the atomic scattering factor in Al and Ni. For the reflections of (006) and (012) in a rhombohedral $LiMO_2$ (M = cation), the structure factor, S, is calculated as $S = 3(f_{Li} + f_M - 2f_O)$. The atomic scattering factors for Li, Al, Ni, and O are 1.77, 8.779, 19, and 5.131, respectively. Thus, S is equal to 0.861/31.524 for α-$LiAlO_2$/$LiNiO_2$. Negligible reflections of (006) and (012) in α-$LiAlO_2$ are expected. (2) The difference in lattice parameters of $LiNiO_2$ and α-$LiAlO_2$. The lattice constants a/c are 2.884 Å/14.19 Å for $LiNiO_2$ and 2.801 Å/14.23 Å for α-$LiAlO_2$, respectively. When the hexagonal setting is used, the corresponding 2θ angles for (018) and (110) reflections are 64.96° and 66.76° for α-$LiAlO_2$. For $LiNiO_2$, reflections of (018) and (110) are closely located at 64.36° and 64.57°. As the content of Al increases, the (006) reflection of XRD shifts to a lower angle, but (110) line shifts to a higher angle. Thus, the splitting of (006) (012) and (018) (110) reflections of Al-doped $LiNiO_2$ was observed. These results indicate that Al-doped $LiNiO_2$ must form a solid solution with Al homogeneously distributed in Ni cation sublattice. The changes in the d-spacing of the reflections are also in good agreement with the substitution of Al for Ni in $LiAl_xNi_{1-x}O_2$ solid solution.

Furthermore, the lattice parameter of $LiAl_xNi_{1-x}O_2$ shows a similar trend as well. Figure 2 shows the hexagonal unit-cell parameters, a- and c-axis, as a function of x in Al-doped $LiNiO_2$. The lattice parameters were refined by a least-squares method. The a-axis decreases linearly from 2.884 to 2.87 Å and the c-axis increases from 14.19 to 14.23 Å. The ratio of c/a increases from 4.92 to 4.96 due to the substitution of Ni ions by Al ions. The unit-cell volume also decreases from 102.22 to 101.45 Å^3 as the content of Al increases. The variation of lattice constant, a, can be expressed as a function of Al content: $a = -0.087x +$
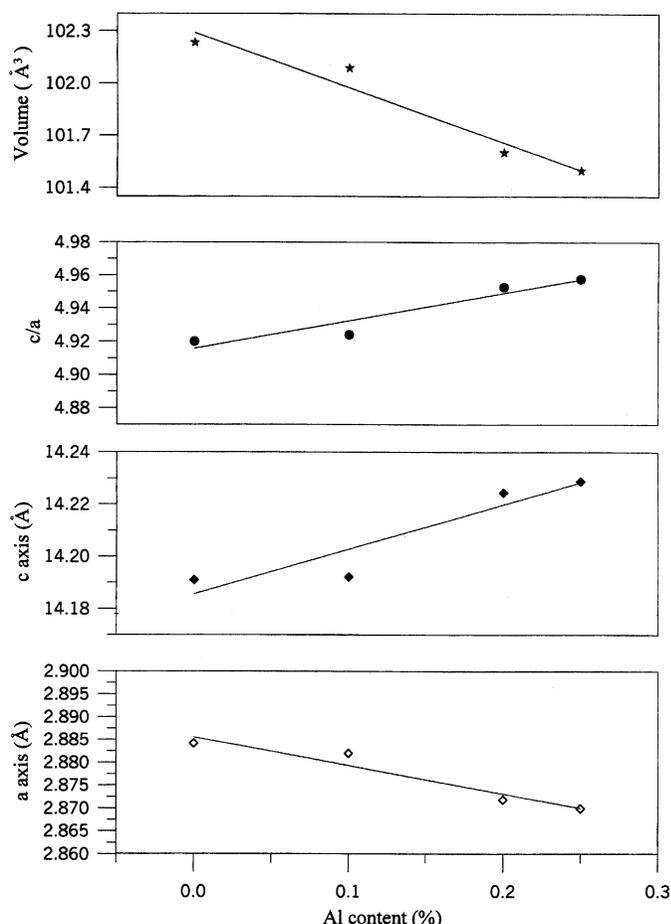
FIG. 2. Lattice parameters of $LiAl_xNi_{1-x}O_2$, a and c, expressed in a hexagonal setting are plotted as a function of Al concentrations.

2.884, ($0 \leq x \leq 0.25$), where x is the concentration of Al in Ni cation sublattice. This result again suggests that the homogeneous substitution of Al in Ni cation sublattice was obtained. The trigonal distortion represented by c/a increases as Al content increases. The result indicates that Al addition favors the stabilization of both Ni^{3+} and the two dimensionality of the crystal lattice. Similar results were reported by Stoyanova et al. (12).

3.2. Reaction Kinetics for the Formation of $LiNiO_2$

3.2.1. Reaction mechanism of $LiNiO_2$. The isothermal reaction of undoped or Al-doped $LiNiO_2$ formation was examined on the basis of the fraction formed, which was determined by integrated intensity from XRD traces. The fraction formed of undoped or Al-doped $LiNiO_2$, α, was plotted as a function of reaction time under isothermal reaction at 650°C, 700°C, and 725°C, respectively. The results for samples doped with various concentrations of
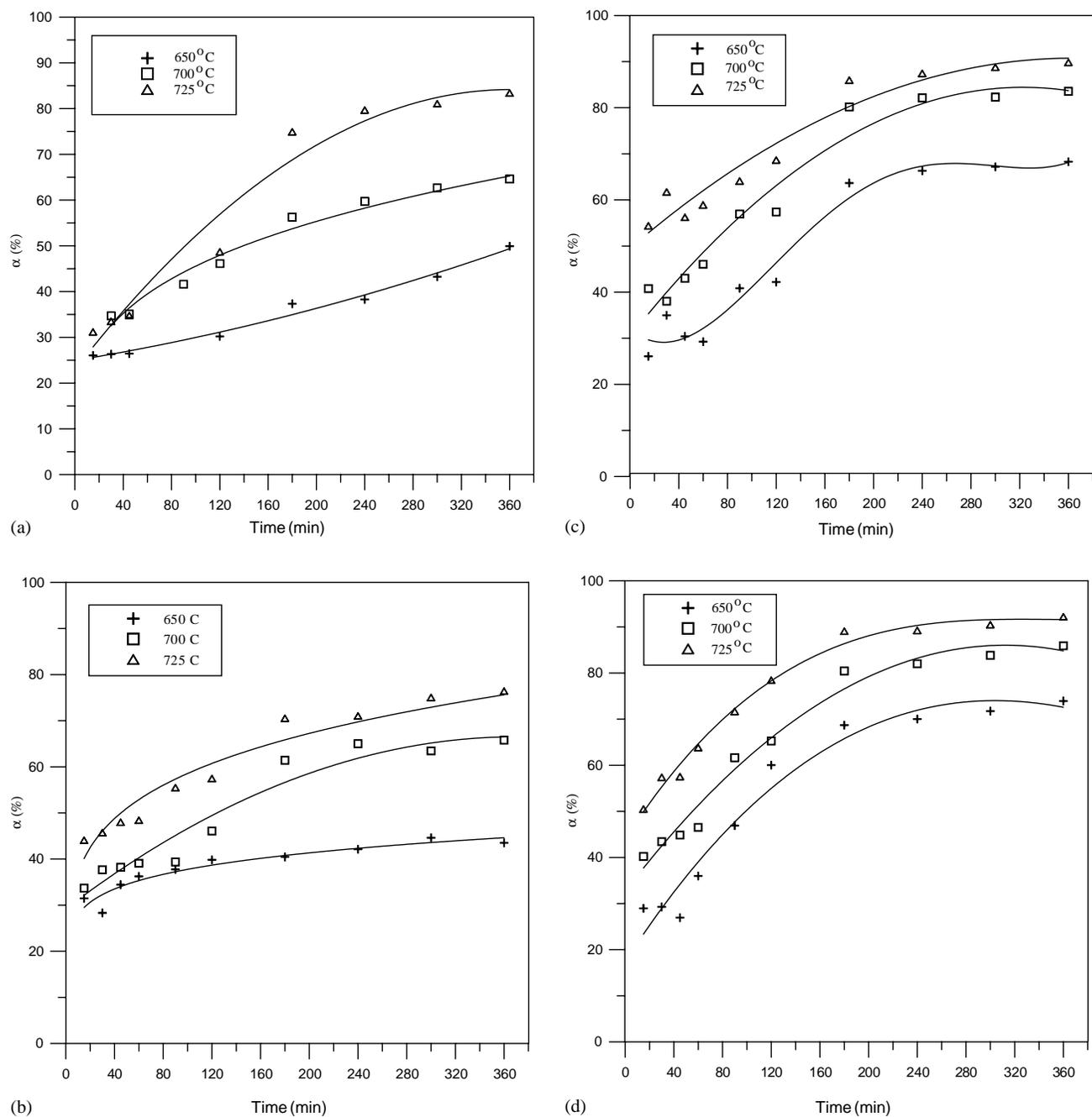
FIG. 3. Fraction of LiAl$_x$Ni$_{1-x}$O$_2$ plotted as a function of reaction time at 650°C, 700°C, and 725°C for various concentrations of Al doping, when x = (a) 0.00, (b) 0.10, (c) 0.20, and (d) 0.25.

Al ($x = 0-0.25$) are shown in Fig. 3, in which, the kinetics result for the synthesis of LiNiO$_2$ from Li$_2$CO$_3$ and NiO follows a parabolic behavior. At 650°C, the fraction formed of LiNiO$_2$ ($x = 0$) was 37% after 180 min reaction. The fraction formed of LiNiO$_2$ increased to 50% when the reaction time was extended to 6 h. The fraction (α) of LiNiO$_2$ also increased as temperature increased. When

temperature was raised to 700°C and 725°C, the fraction of LiNiO$_2$ reached 50% within 150 and 120 min, respectively.

The formation of undoped LiNiO$_2$ can be expressed by the Ohlberg–Strickler equation (14–20):

$$\alpha = 1 - \exp(-Bt^m), \qquad [1]$$

$$-\ln \ln(1 - \alpha) = \ln B + m \ln t, \qquad [2]$$

where α is the fraction transformed, B is a constant depending upon the nucleation frequency and linear rate of grain growth, and m is the Avrami constant depending upon the reaction mechanism and the geometry of the system (16). By plotting $-\ln \ln(1-\alpha)$ as a function of $\ln t$, the value of m was determined from the value of the slope. This expression has been widely described in the solid-state reaction for many material systems such as $BaTiO_3$,

MgO–SiO_2, and some superconductors. For the formation of $LiNiO_2$, the Avrami constant, m, was determined to be around 0.54 based on the slopes shown in Fig. 4. These results indicate that the reaction mechanism is a diffusion-controlled process, which is also in agreement with the model of 3D growth (14–15).

The SEM micrographs for $LiNiO_2$ calcined at 700°C for 36 h are shown in Fig. 5(a). The micrograph shows cubic and spherical grain of $LiAl_xNi_{1-x}O_2$, which is typical for 3-D geometric growth.
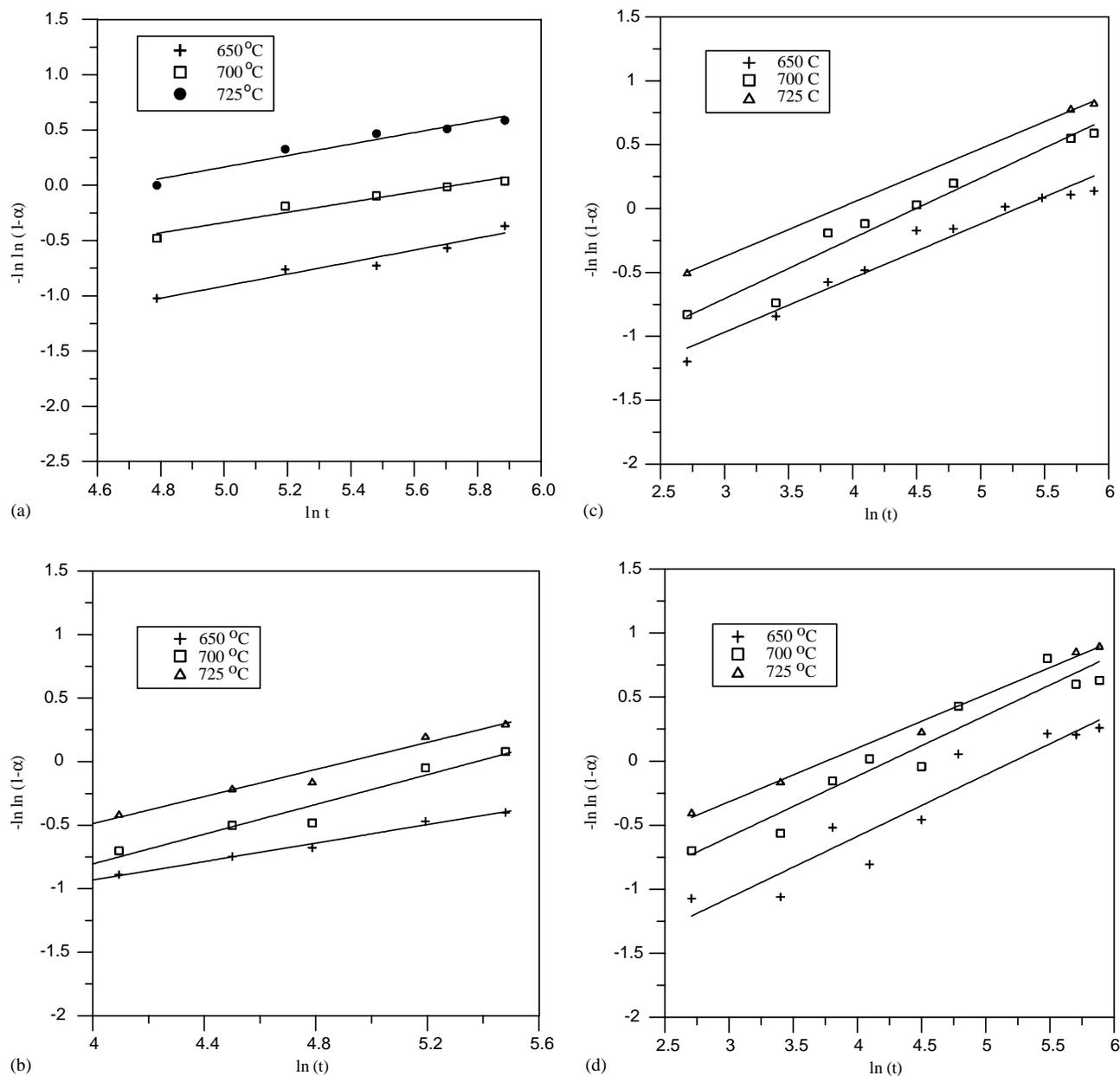
FIG. 4. The determination of the Avrami constant m in the crystallization process for $LiAl_xNi_{1-x}O_2$, when $x =$ (a) 0.00, (b) 0.10, (c) 0.20, and (d) 0.25.
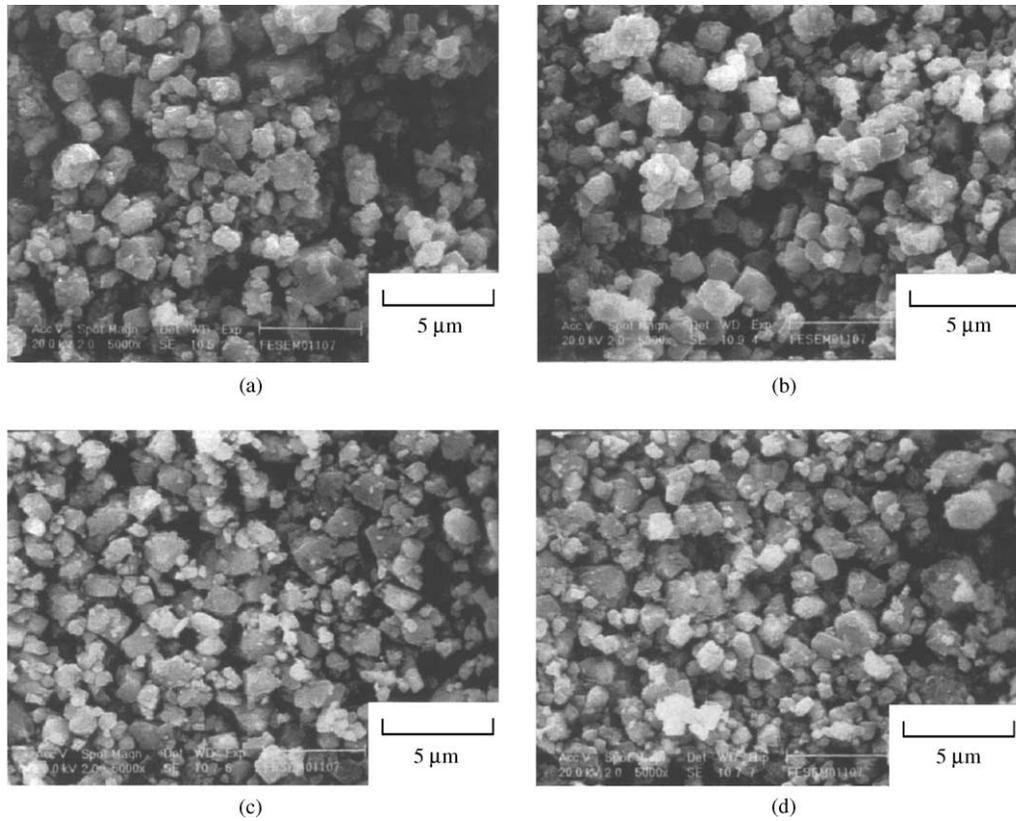
FIG. 5. SEM micrographs for the LiAl$_x$Ni$_{1-x}$O$_2$ powders calcined for 36 h in O$_2$ atmosphere, when $x =$ (a) 0.00, (b) 0.10, (c) 0.20, and (d) 0.25.

3.2.2. Rate constant for the formation of LiNiO$_2$. The reaction mechanism can be further represented using a model of geometric growth which was described by Jander (15, 21, 22):

$$[1 - (1 - \alpha)^{1/3}]^2 = Kt. \qquad [3]$$

To determine the rate constant, K in the Jander model, the $[1 - (1 - \alpha)^{1/3}]^2$ was plotted as a function of t at various temperatures as shown in Fig. 6. The K values for the formation of LiAl$_x$Ni$_{1-x}$O$_2$ ($x = 0-0.25$) at various temperatures were obtained from the slopes shown in Fig. 6. Figure 7 shows the variation of rate constant K, as a function of $1/T$. The result indicates that such a reaction is a thermally activated process and can be expressed by the following equation:

$$K = K_0 \exp(-E_a/RT), \qquad [4]$$

where K_0 is a pre-exponential constant; E_a the activation energy; R the gas constant; and T the absolute temperature.

The activation energy for the formation of LiNiO$_2$ was determined from the slope of the straight line fitted through data points.

3.2.3. Effect of Al addition on the kinetics of LiNiO$_2$ formation. For undoped mixture of Li$_2$CO$_3$ and NiO, the activation energy for the formation of undoped LiNiO$_2$ was found to be as high as 190 kJ/mol. It was observed that the fraction (α) of LiNiO$_2$ was significantly enhanced by the addition of Al. For example, the fraction of LiNiO$_2$ reached 50% within 2.5 h and 1 h when 25% of Ni was substituted by Al.

The Avrami constant, m, determined from Figs. 4(b)–(d) also shows a value of 0.54 which suggests that the reactions are diffusion controlled. However, the rate constant determined from Jander model was enhanced by the addition of Al. When Al ions were added into the mixture of Li$_2$CO$_3$ and NiO, the activation energy for LiNiO$_2$ formation was significantly affected. For the addition of 10% Al, the activation energy decreased slightly to 189 kJ/mole. However, when the concentration of Al increased to 20% and 25%, the activation energy drastically reduced to 95 and 83 kJ/mole, respectively. The decrease in the activation energy suggests that the energy barrier for the formation of LiNiO$_2$ is effectively suppressed by the addition of Al ions. Therefore, the reaction kinetics of LiNiO$_2$ formation was
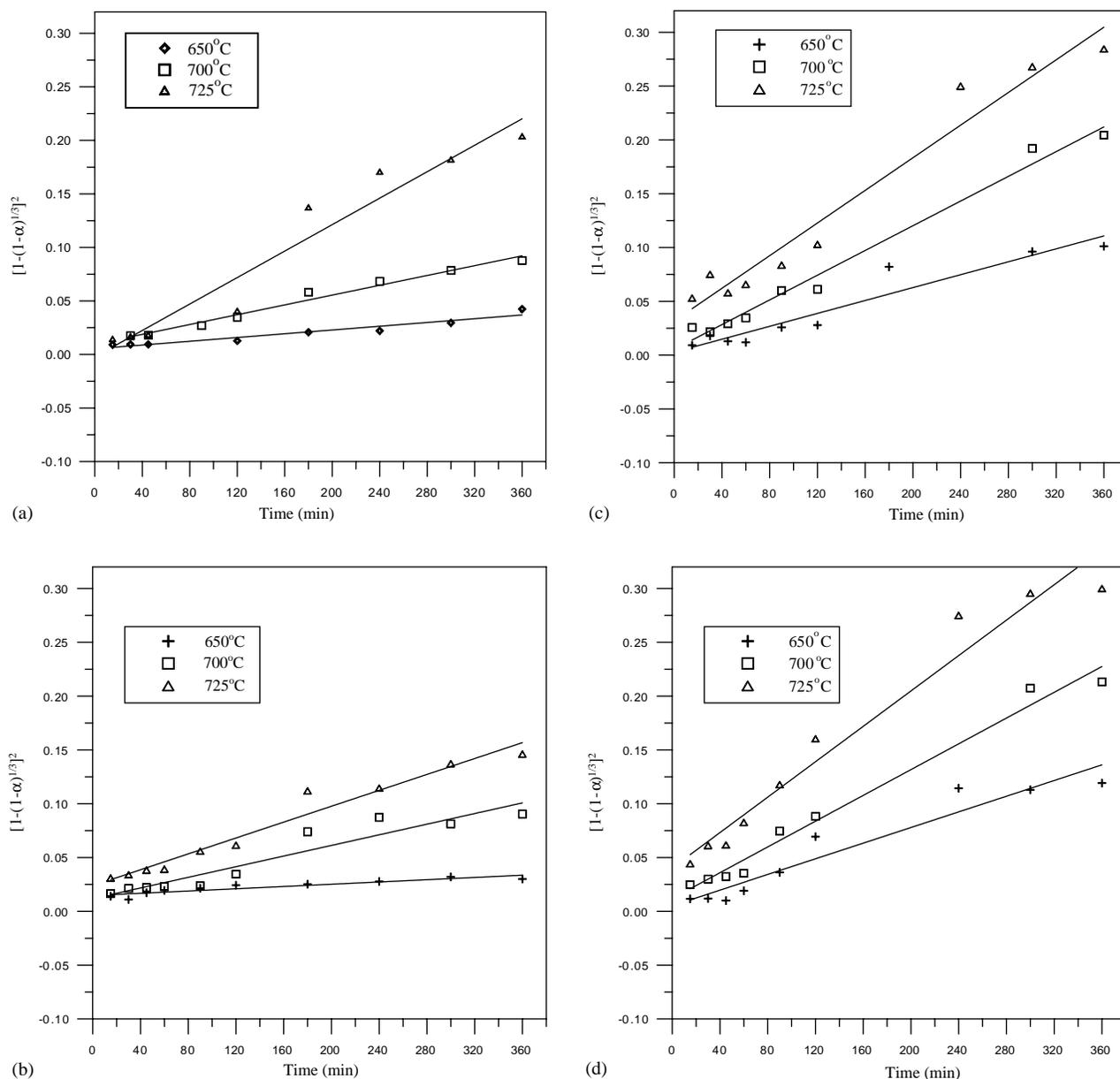
FIG. 6. The plots of $[1 - (1 - \alpha)^{1/3}]^2$ vs t for the formation of $LiAl_xNi_{1-x}O_2$ at 650°C, 700°C, and 725°C, when $x =$ (a) 0.00, (b) 0.10, (c) 0.20, and (d) 0.25.

enhanced by the incorporation of Al ions into the lattice of $LiNiO_2$.

3.3. Role of Al in the Formation of $LiNiO_2$

According to the results shown in previous sections, the substitution of Al in Ni cation sublattice enhanced the formation of $LiNiO_2$. It is important to examine the role of Al in the enhancement of $LiNiO_2$ formation. In our previous work (15), it was suggested that the formation

of $LiNiO_2$ using solid-state reaction method was controlled by the diffusion of Ni cations. Thus, the activation energy of 190 kJ/mole observed was close to that for the formation of Ni vacancies, as described by the following defect reaction:

$$1/2\,O_{2(g)} \xrightarrow[NiO]{} 2h^\cdot + V''_{Ni} + O_O^x. \qquad [5]$$
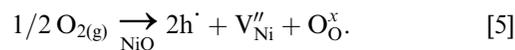
As shown previously, the reduction of activation energy from 190 to 95 and 83 kJ/mole was apparently caused by the addition of 20% and 25% Al, respectively.
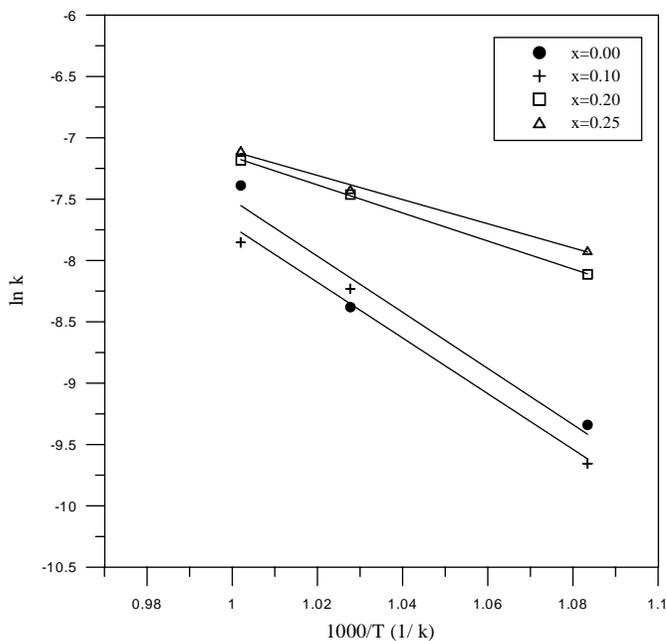
FIG. 7. The plot of ln K vs $1000/T$ for the formation of LiAl$_x$Ni$_{1-x}$O$_2$ when x varied from 0.00 to 0.25.

The possible reactions for Al with the mixture of Li$_2$CO$_3$ and NiO may take place by the following routes:

(1) *Formation of solid solution* Al$_x$Ni$_{1-x}$O: such a reaction may be expressed by

$$Al_2O_3 \xrightarrow[NiO]{} 2Al^{\cdot}_{Ni} + V''_{Ni} + 3O^x_O. \quad [6]$$
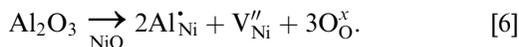
Thus, the cation diffusion may be enhanced by the formation of solid solution Al$_x$Ni$_{1-x}$O.

(2) *Formation of α-LiAlO$_2$*: Aluminum and lithium oxides can easily form stable lithium aluminate at a temperature as low as 500°C.

Thus, to determine the role of Al in the formation of LiNiO$_2$, further examination was needed. In order to distinguish the influence of Al$_x$Ni$_{1-x}$O and α-LiAlO$_2$ on the formation of Al-doped LiNiO$_2$, three reactions with different starting materials were studied.

(i) *Reaction A*: The starting materials used were Li$_2$CO$_3$, α-LiAlO$_2$, and NiO in a molar ratio of 49:2:98.

(ii) *Reaction B*: The starting materials used were Li$_2$CO$_3$ and Al$_{0.02}$Ni$_{0.98}$O in the molar ratio of 1:2.

(iii) *Reaction C*: The starting materials were Li$_2$CO$_3$ and NiO in a molar ratio of 1:2.

After reaction at 700°C for various periods of time, the fraction formed of layered LiNiO$_2$ for the above-mentioned reactions is shown in Fig. 8. After heating at 700°C for 60 min, the reaction A with the addition of α-LiAlO$_2$ obtained more LiNiO$_2$ than the other ones especially in the early stage of the reaction. For the undoped reaction C, the initial reaction was sluggish. The

addition of Al$_{0.02}$Ni$_{0.98}$O solution, the reaction B, however, exhibits much slower kinetics than reactions A and C. These results suggest that α-LiAlO$_2$ enhanced but Al$_{0.02}$Ni$_{0.98}$O suppressed the formation of LiNiO$_2$ in comparison with reaction C.

3.3.1. Kinetics suppression by Al$_{0.02}$Ni$_{0.98}$O. The suppression of reaction B by Al$_{0.02}$Ni$_{0.98}$O can be rationalized by the substitution of Ni for Al in NiO. For the formation of LiNiO$_2$ from Li$_2$O and NiO, the following defect reaction may occur:

$$\tfrac{1}{2}O_2 + Li_2O + 2NiO \xrightarrow[NiO]{} 2Li'_{Ni} + 2h^{\cdot} + 2Ni^x_{Ni} + 4O^x_o. \quad [7]$$
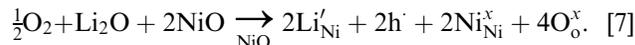
For Eq. [7] to proceed, the availability of Ni cation with +2 valence is required.

With the formation of Al$_{0.02}$Ni$_{0.98}$O solid solution, Al ions occupy Ni positions and create cation vacancies as shown in Eq. [6]. In addition, when Li$_2$O reacts with Al$_{0.02}$Ni$_{0.98}$O, Li ions may fill up the available cation vacancies instead of forming Ni^{3+}. Such a reaction may be described by

$$Li_2O + V''_{Ni} \xrightarrow[NiO]{} 2Li'_{Ni} + O^x_o. \quad [8]$$
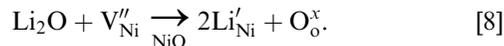
With less Ni^{3+} created in NiO structure, the formation of layered LiNiO$_2$ tends to be sluggish.
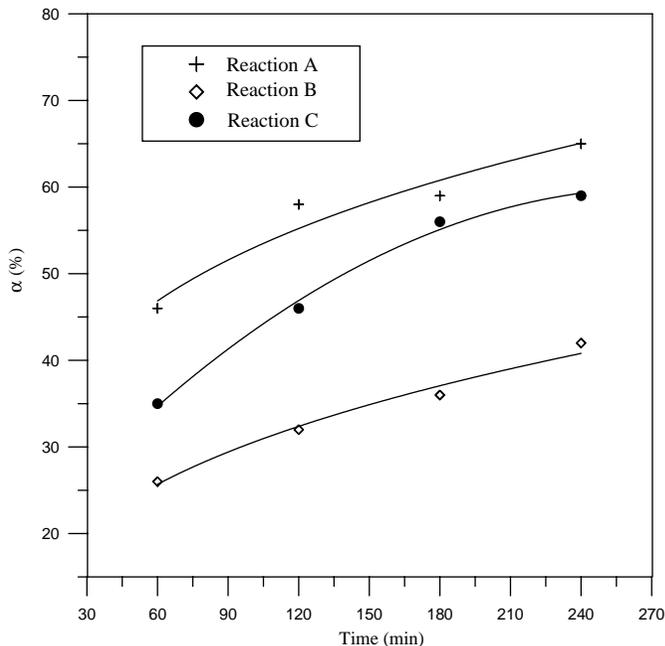
FIG. 8. Fractions formed of undoped and Al-doped LiNiO$_2$ are plotted as a function of reaction time at 700°C when various starting materials were used, where the reaction C was used as a standard: (A) 0.49Li$_2$CO$_3$ + 0.02 α-LiAlO$_2$ + 0.98NiO; (B) 0.5Li$_2$CO$_3$ + Al$_{0.02}$Ni$_{0.98}$O; and (C) LiNiO$_2$: 0.5Li$_2$CO$_3$ + NiO.

3.3.2. Kinetics enhancement by α-LiAlO₂. On the contrary, the presence of LiAlO₂ in the powder mixture enhances the formation of LiNiO₂. In order to investigate the role of α-LiAlO₂ in the enhancement of LiNiO₂ formation, various amounts of α-LiAlO₂ were added into the mixture of Li₂CO₃ and NiO. The results are shown in Figs. 9 and 10.

The kinetics were greatly enhanced in the beginning of isothermal reaction as shown in Fig. 8. Without the addition of α-LiAlO₂, considerable amounts of Li₂CO₃ and lithated-NiO were still observed, Fig. 9(a). Again, a sluggish reaction for the formation of undoped LiNiO₂ was observed. It is believed that α-LiAlO₂ with rhombohedral structure acts as the seeding material for the formation of LiNiO₂.

After adding different amounts of α-LiAlO₂ into the mixture of Li₂CO₃ and NiO, the reflections in XRD representing LiNiO₂ appeared, and its fraction was calculated as shown in Fig. 10, in which more LiNiO₂ was formed when the concentration of α-LiAlO₂ increased.

Fig. 9(e) shows the XRD trace for LiAlO₂ heated at 725°C for 2 h. Both γ-LiAlO₂ and α-LiAlO₂ coexisted.
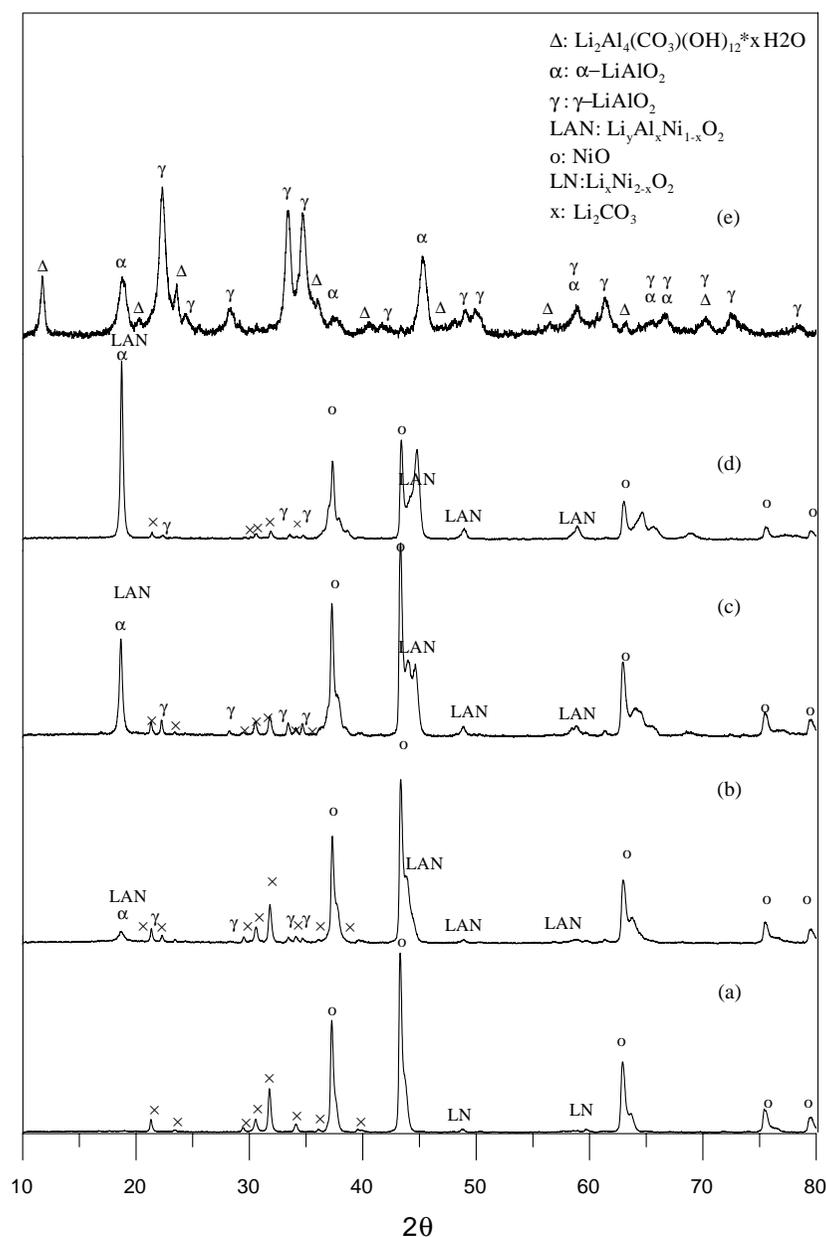
FIG. 9. The XRD patterns of compound synthesized at 725°C for 2 h using α-LiAlO₂, NiO and Li₂CO₃ as starting materials. Various amounts of α-LiAlO₂ were used as (a) 0.00, (b) 0.10, (c) 0.20, (d) 0.25, and (e) 1.00.
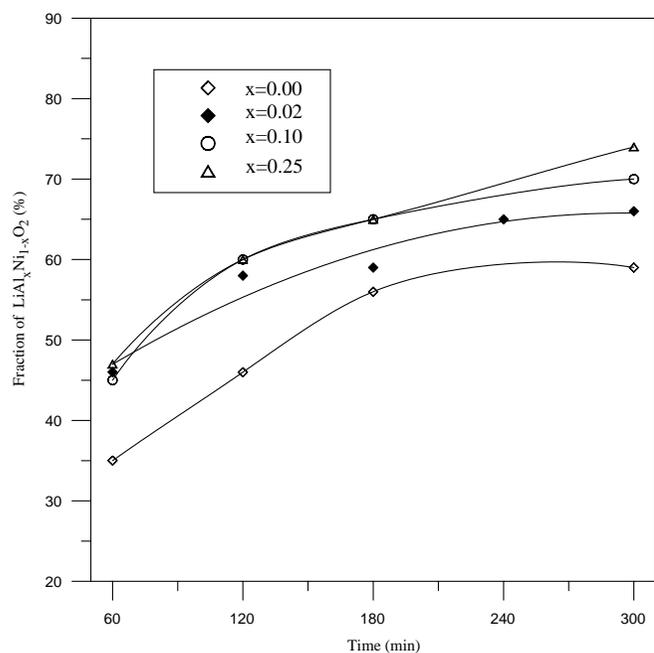
FIG. 10. Fractions of LiAl$_x$Ni$_{1-x}$O$_2$ formed plotted as a function of reaction time at 700°C, when x varied from 0.00 to 0.25.

γ-LiAlO$_2$ is known as the high-temperature phase which appears at temperatures greater than 600°C. In Fig. 9(b)–9(d), the fact that only a small amount of γ-LiAlO$_2$ was observed suggests that most of α-LiAlO$_2$ has indeed participated in the formation of LiNiO$_2$. The enhancement of α-LiAlO$_2$ in the formation of LiNiO$_2$ is attributed to similar crystal structures. Once the lithiation of NiO proceeded and the structure deviated from NaCl-type structure to rhombohedral structure, the solid solution between LiNiO$_2$ and α-LiAlO$_2$ would be formed easily. The role of α-LiAlO$_2$ acts as the seeding material which provides nucleation site for the growth of LiNiO$_2$. Therefore, the activation energy for this reaction can be significantly reduced by the addition of Al or α-LiAlO$_2$.

4. CONCLUSIONS

Based on the results of this work, the following conclusions may be drawn:

1. Using solid-state reaction method, the formation of LiNiO$_2$ from Li$_2$CO$_3$ and NiO reaction is sluggish. For example, 150 min of reaction time was needed to obtain 50% of LiNiO$_2$ at 700°C.

2. With the addition of Al into the mixture of Li$_2$CO$_3$ and NiO, the formation of Al-doped LiNiO$_2$ was significantly enhanced. When the reaction temperature was kept at 700°C, 50% of Al-doped LiNiO$_2$ was obtained in about 60 min.

3. The activation energy for the formation of LiNiO$_2$ was also suppressed by the addition of Al. With the addition of 25% Al, the activation energy estimated was only 83 kJ/mole, compared with 190 kJ/mole for undoped LiNiO$_2$.

4. The faster kinetics for the formation of Al-doped LiNiO$_2$ may be due to the similar structure between LiNiO$_2$ and α-LiAlO$_2$. When the dissolution between α-LiAlO$_2$ and lithiated NiO occurs, Al^{3+} substitution for Ni may further enhance the cation diffusion and reaction.

REFERENCES

1. G. Dutta, A. Manthiram, and J. B. Goodenough, *J. Solid State Chem.* **96,** 123 (1992).
2. M. Tabuchi, K. Ado, H. Kobayashi, H. Sakaebe, H. Kageyama, C. Masquelier, M. Yonemura, A. Hirano, and R. Kanno, *J. Mater. Chem.* **9,** 199 (1999).
3. C. H. Lu and P. Y. Yeh, *J. Mater. Chem.* **10,** 599 (2000).
4. M. T. Le, J. Gaubicher, E. Bermejo, Y. Chabre, and M. Quarton, *J. Mater. Chem.* **9,** 567 (1999).
5. S. P. Lin, K. Z Fung, Y. M. Hon, and M. H. Hon, *J. Cryst. Growth* **226,** 148 (2001).
6. O. Zhong and U. V. Sacken, *J. Power Sources* **54,** 221 (1995).
7. T. Ohzuku, A. Ueda, and M. Kouguchi, *J. Electrochem. Soc.* **142,** 4033 (1995).
8. H. A. Lehmann and H. Hesselbarth, *Z. Anorg. Allg. Chem.* **313,** 117 (1961).
9. K. R. Poppelmeter, C. K. Chiang, and D. O. Kipp, *Inorg. Chem.* **27,** 4523 (1988).
10. M. K. Aydinol, A. F. Kohan, G. Ceder, K. Cho, and J. Joannopoulos, *Phys. Rev. B* **56,** 1354 (1997).
11. Y. Jang, B. Huang. H. Wang, G. R. Maskaly, G. Ceder, D. R. Sadoway, Y. M. Chiang, and H. Tamura, *J. Power Sources* **81–82,** 589 (1999).
12. R. Stoyanova, E. Zhecheva, E. Kuzmanova, R. Alcantara, P. Lavela, and J. L. Tirado, *Solid State Ionics* **128,** 1 (2000).
13. S. I. Pyun, *J. Power Sources* **81–82,** 442 (1999).
14. S. M. Ohlberg and D. W. Strickler, *J. Am. Ceram. Soc.* **45,** 171 (1962).
15. S. P. Lin, K. Z Fung, Y. M. Hon, and M. H. Hon, *J. Cryst. Growth* **234,** 176 (2001).
16. J. D. Hankcock and J. H. Sharp, *J. Am. Ceram. Soc.* **55,** 74 (1972).
17. J. Beretka, *J. Am. Ceram. Soc.* **67,** 615 (1984).
18. J. H. Sharp, G. W. Brindley, and B. N. Narahari Achar, *J. Am. Ceram. Soc.* **49,** 379 (1966).
19. J. H. Taplin, *J. Am. Ceram. Soc.* **57,** 140 (1974).
20. R. E. Carter, *J. Chem. Phys.* **34,** 2010 (1961).
21. W. Jander, *Z. Anorg. Allg. Chem.* **163,** 1 (1927).
22. S. P. Mitoff, *J. Chem. Phys.* **35,** 882 (1961).